Journal of Experimental Botany, Vol. 62, No. 10, pp. 3637–3645, 2011
doi:10.1093/jxb/err065 Advance Access publication 17 March, 2011

Journal of Experimental Botany
www.jxb.oxfordjournals.org

RESEARCH PAPER

Relationship between ultrasonic properties and structural changes in the mesophyll during leaf dehydration

Domingo Sancho-Knapik[1], Tomás Gómez Álvarez-Arenas[2], José Javier Peguero-Pina[3], Victoria Fernández[4] and Eustaquio Gil-Pelegrín[1,*]

[1] Unidad de Recursos Forestales, Centro de Investigación y Tecnología Agroalimentaria, Gobierno de Aragón, E-50059, Zaragoza, Spain
[2] Grupo de Señales, Sistemas y Tecnologías Ultrasónicas., CSIC, E-28002 Madrid, Spain
[3] Departament de Biologia, Universitat de les Illes Balears, Carretera de Valldemossa, km 7.5, E-07071 Palma de Mallorca, Balears, Spain
[4] Forest Genetics and Ecophysiology Research Group, ETS Forest Engineering, Technical University of Madrid, Ciudad Universitaria s/n, E-28040 Madrid, Spain

* To whom correspondence should be addressed. E-mail: egilp@aragon.es

Received 2 December 2010; Revised 20 January 2011; Accepted 15 February 2011

Abstract

The broad-band ultrasonic spectroscopy technique allows the determination of changes in the relative water content (RWC) of leaves with contrasting structural features. Specifically, the standardized frequency associated with the maximum transmittance (f/f_o) is strongly related to the RWC. This relationship is characterized by the existence of two phases separated by an inflexion point (associated with the turgor loss point). To obtain a better understanding of the strong relationship found between RWC and f/f_o, this work has studied the structural changes experienced by *Quercus muehlenbergii* leaves during dehydration in terms of ultrasounds measurements, cell wall elasticity, leaf thickness, leaf density, and leaf structure. The results suggest that the decrease found in f/f_o before the turgor loss point can be attributed to the occurrence of changes in the estimation of the macroscopic effective elastic constant of the leaf (c_{33}), mainly associated with changes in the bulk modulus of elasticity of the cell wall (ε). These changes are overriding or compensating for the thickness decreases recorded during this phase. On the other hand, the high degree of cell shrinkage and stretching found in the mesophyll cells during the second phase seem to explain the changes in the acoustic properties of the leaf beyond the turgor loss point. The formation of large intercellular spaces, which increased the irregularity in the acoustic pathway, may explain the increase of the attenuation coefficient of ultrasounds once the turgor loss point threshold is exceeded. The direct measurement of c_{33} from ultrasonic measurements would allow a better knowledge of the overall biomechanical properties of the leaf further than those derived from the P–V analysis.

Key words: Cell wall elasticity, leaf thickness, relative water content, turgor loss point, ultrasonic spectroscopy, water potential.

Introduction

The broad-band ultrasonic spectroscopy technique has been proven as a non-destructive, non-invasive, non-contact, and reproducible method for the dynamic determination of leaf water status. It is based on the excitation of thickness resonances on the leaves, specifically, changes in the standardized frequency (f/f_o) at the maximum transmittance (leaf resonant condition). This parameter has been revealed as an optimum indicator of the relative water content (RWC) of leaves with contrasting structural features (Gómez Álvarez-Arenas *et al.*, 2009*a*). The relationship between f/f_o and RWC is characterized by the existence of two phases separated by an inflexion point, which has been

Abbreviations: c_{33}, macroscopic effective elastic constant; ε, bulk modulus of elasticity of the cell wall; f/f_o, standardized frequency; P–V curves, pressure–volume curves; RWC, relative water content; Ψ, water potential; TLP, turgor loss point.

associated with the turgor loss point (Sancho-Knapik *et al.*, 2010).

The existence of two phases in the physics of leaf dehydration was firstly reported by Tyree and Hammel (1972) regarding the analysis of the leaf P–V relationships. During the first phase, when the leaf is water-saturated (RWC=1.00), the protoplast of the cell exerts a positive pressure over the cell wall, which is maximally distended (maximum turgor pressure) (Tyree and Jarvis, 1982). Loss of water during the first phase, which is modulated by the elasticity of the cell wall, leads to a reduction in the cellular volume and, as a consequence, to a direct decrease in the pressure over the cell wall. The cell volume progressively diminishes until a threshold value, beyond which the protoplast does not exert pressure over the cell wall (Larcher, 2003; Pritchard, 2007).

During this first phase, before the turgor loss point, Sancho-Knapik *et al.* (2010) reported a decrease in flf_o when the leaf is dehydrated. According to Temkin (1981), the resonant frequency of an elastic plate, when wave dispersion phenomena can be considered negligible, is given by the following equation:

$$f = v_z/2l \quad (1)$$

where f is the resonant frequency, v_z is the velocity of the ultrasonic longitudinal wave in the leaf along the direction normal of the leaf plane (z-axis) and l is the leaf thickness (Gómez Álvarez-Arenas *et al.*, 2003*a*). This velocity, which is dependent on elastic constants of the measured material (Auld, 1990), is given by:

$$v_z = (c_{33}/\rho)^{1/2} \quad (2)$$

where c_{33} is the macroscopic effective elastic constant of the material for compression waves in the z direction and ρ is the density (Auld, 1990). c_{33} determines the bulk macroscopic elastic stiffness of the material in the z direction. The relationship between c_{33} and the microscopic features of a material is not straightforward. In composites, for example, c_{33} depends on the components, their volumetric concentration and spatial distribution (Christensen, 2005). In foams, there are several mechanisms that contribute to furnish the overall response of c_{33} (e.g. compression and bending of the struts) (Gibson and Ashby, 1997). In this sense, it could be expected that the macroscopic c_{33} of plant leaves can be the result of a number of contributions. Among them, the effect of the tissue stiffness can be assessed independently by comparing c_{33} with the bulk modulus of elasticity (ε) calculated from the P–V curves. Therefore, it is expected that the reduction of ε may cause a variation of c_{33}. This fact will cause a variation in v_z (equation 2) and, as a consequence, the reduction in f, which will be consistent with the experimental data showed by Gómez Álvarez-Arenas *et al.* (2009*a*).

In addition, the loss of turgor may produce a decrease of the leaf thickness (Burquez, 1987) and a slight increase in leaf density (Ogaya and Peñuelas, 2006). These changes in leaf anatomical properties may have an influence on the resonant frequency at the higher values, according to equations 1 and 2. However, the shift of the resonant frequency towards lower values (Gómez Álvarez-Arenas *et al.*, 2009*a*) suggests that the changes in c_{33} exert a dominant effect over the changes in the leaf resonant frequency during this first phase.

Once the turgor loss point is exceeded, a new phase starts in the leaf dehydration process, which is characterized by the absence of cell turgor. Thus, it is assumed that cell walls are not under positive pressure during this phase (Tyree, 1976; Pritchard, 2007). Therefore, changes in pressure can no longer determine the variation of the acoustic properties of the leaf observed after the turgor loss point. Subsequent leaf dehydration increases the concentration of the sap cell, inducing changes in the osmotic potential and, as a consequence, in the water potential of the whole cell (Mitchell *et al.*, 2008). These physiological adjustments may induce morphological changes in the mesophyll cells of the leaf. In this way, it has been suggested that, at this point, the cell walls are drawn inward and may shrivel (Larcher, 2003). These conformational changes may be similar to the elastic buckling found in cellular solids subjected to a strong compression (Gibson and Ashby, 1997). It is known that the elastic buckling causes a decrease in c_{33}, which could explain the further decrease found in the resonant frequency beyond the turgor loss point. On the other hand, an additional effect to these conformational changes is the formation of gas-filled spaces in the internal tissues, which could be explained by the lateral shrinkage of mesophyll cells, as shown by Cryo-SEM observations of dehydrated leaf tissues (McBurney, 1992). Thus, the strong increase in the leaf internal heterogeneity during this phase may underlie the change in the acoustic properties of the leaf, which are associated with an increase in signal attenuation (Sancho-Knapik *et al.*, 2010).

Therefore, the main objective of this work is to study in depth the structural changes experimented by the leaf during dehydration, in order to obtain a better understanding for the strong relationship found between RWC and flf_o, interpreting the ultrasonic measurements in terms of leaf structure, composition and water status. For this purpose, the changes occurring during different leaf dehydration steps were assessed in terms of ultrasounds measurements, P–V analysis, leaf thickness, and leaf structure.

Materials and methods

Plant material and experimental conditions

Measurements were carried out in ten mature leaves collected from *Quercus muehlenbergii* Engelm, the species selected for this study. In the early morning, branches were collected from the north side of the trees, placed in plastic bags and carried out to the laboratory. Once there, leaf petioles were re-cut under water to avoid embolism and kept immersed (avoiding the wetting of leaves) for 24 h at 4 °C until full leaf rehydration. It was considered that over-rehydration did not take place because changes in leaf optical properties were not observed (i.e. dark spots or dark areas in the leaf lamina). After 24 h, weight and

ultrasonic parameters were individually measured per leaf at constant time intervals following the methodology described in Gómez Álvarez-Arenas *et al.* (2009*a*) and Sancho-Knapik *et al.* (2010). Leaves were weighed and measured at different levels of RWC, starting at full saturation (turgid weight, TW). Leaf dry weight (DW) was estimated after keeping the plant material in a stove (24 h, 60 °C). The RWC was then calculated following the expression: RWC=(FW–DW)/(TW–DW), FW being the sample fresh weight at any moment.

P–V analysis

P–V relationships were determined following the free-transpiration method described in previous studies (Clifford *et al.*, 1998; Corcuera *et al.*, 2002; Burghardt and Riederer, 2003; Vilagrosa *et al.*, 2003). The water relations parameters analysed were leaf water potential at the turgor loss point, Ψ_{TLP}; maximum bulk modulus of elasticity, ε_{max}; maximum turgor, π; and the relative water content at the turgor loss point, RWC_{TLP}. The symplastic water loss (RWL, %) was calculated in order to obtain the Höfler diagram. Moreover, the dynamic changes in the bulk modulus of elasticity (ε) associated to changes in turgor pressure were analysed.

Leaf thickness and leaf density measurements

Leaf thickness was determined using a digital contact sensor GT-H10L coupled to an amplifier GT-75AP (GT Series, Keyence Corporation, Japan). This ultra-low force sensor (having a measuring force of 0.2 N when installed facing up) applies a clamp pressure of 7 kPa, which is *c*. ten times lower than the one used by Zimmermann *et al.* (2008) for a similar purpose. Thereby, it is ensured that determinations did not disturb leaf thickness measurements due to an excess of pressure over the leaf. The loss of thickness per leaf is expressed as the ratio between the thickness measured for every particular RWC and the thickness determined at full turgor.

Leaf density (ρ, kg m^{-3}) was calculated by measuring, in another set of leaves, the variation in leaf area, thickness, and weight during the dehydration process. In addition to the other parameters already mentioned, the area was obtained through the realization of digital images of the leaves and posterior analysis using the public domain NIH Image program (developed at the US National Institutes of Health and available at http://rsb.info.nih.gov/nih-image/). The volume of the leaf was calculated as the product between the leaf thickness and the area. ρ was then obtained as the ratio between leaf weight and leaf volume.

Cryo-scanning elecron microscopy (SEM) observations

Quercus muehlenbergii leaves at three different RWC levels (i.e. at full turgor, around the turgor loss point, and at a RWC of *c*. 0.72) were observed with a low temperature scanning electron microscope (LTSEM, DSM 960 Zeiss, Germany, acceleration potential 15 kV, working distance 10 mm and probe current 5–10 nA). Fresh transverse sections were frozen in liquid N, gold sputtered and subsequently observed by this microscopic technique. Micrographs were analysed using the public domain NIH Image program (developed at the US National Institutes of Health and available at http://rsb.info.nih.gov/nih-image/). The length and width of the 20 palisade and 20 spongy parenchyma cells were measured at the three different RWC levels studied.

The broad-band ultrasonic spectroscopy technique: experimental set-up and parameters measured

The experimental set-up consists of two pairs of specially designed air-coupled piezoelectric transducers (Fig. 1A); in this case with a centre frequency of 0.75 MHz, a working frequency range of 0.3–1.2 MHz, and with a radiating diameter area of 20 mm (Gómez

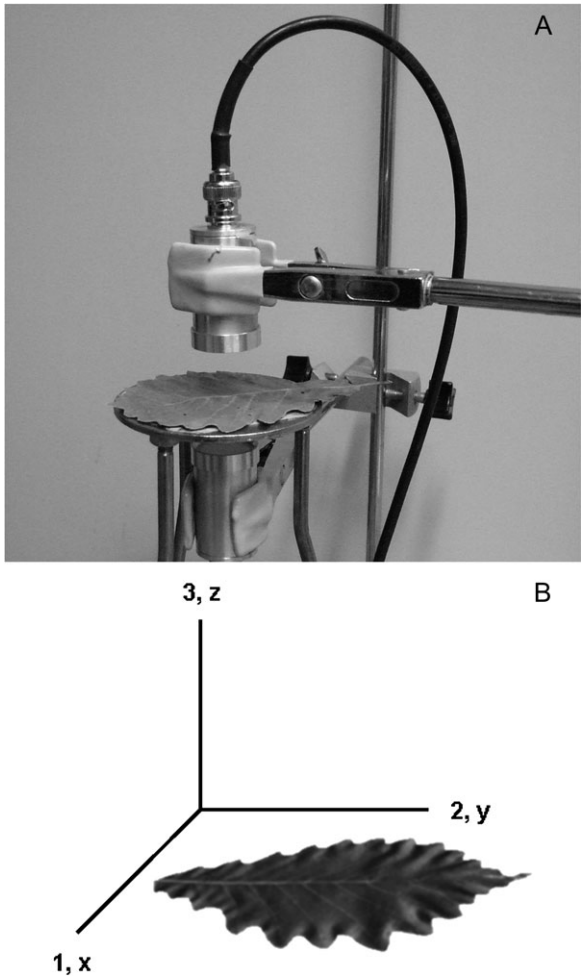

Fig. 1. Experimental set-up (A) and reference frame for the assessment of the measurements of the leaf rigidity (B).

Álvarez-Arenas, 2003*a*, 2004). These transducers are positioned facing each other at a distance of 2 cm. A high voltage (100–400 V) square semicycle (duration of 0.67 μs) is applied with a Panametrics 5077 pulser-receiver (Olympus, USA) to the transmitter transducer which converts this electrical signal into an ultrasonic pulse and launches it into the air. The receiver transducer collects this signal and converts it into an electrical one, then it is amplified (up to 59 dB) and filtered (low-pass filter at 10 MHz). Eventually, an oscilloscope (Tektronix 5052 TDS, Tektronix Inc., USA) digitize it, average a number of waveforms to reduce the high frequency noise (typically up to 100 waveforms), perform the Fast Fourier Transform (FFT) and transfer the data to a computer for storage. The sample rate of the oscilloscope was set to 25 Ms s^{-1} with a total length of 5000 points. The experimental procedure of the ultrasonic technique is as follows. First, transmission from a transmitter is directly measured into the receiver, providing a calibration of the system. Then a leaf is held for a few seconds between the transducers at normal incidence. When the ultrasounds impact normally on the leaf surface, part of the energy is transmitted through the leaf, and reaches the back surface. Then part of the energy is transmitted through the interface (air) and received at the receiver transducer.

The ultrasonic parameter directly measured was the transmitted pulse in the time domain. The Fourier transformation enabled obtaining a transmittance (T) versus frequency curve for each output. The value of the frequency associated with the maximum T at the peak curve was compared to the relative water content (RWC). The frequency values were standardized (f/f_o) by means of

dividing each single value (f) by the maximum value obtained at RWC=1.00 (f_o) for each leaf studied (Sancho-Knapik *et al.*, 2010). Moreover, to estimate the attenuation of sound in the samples, the inverse of the quality factor (Q) was employed, since $1/Q$ is directly proportional to it. An increase in $1/Q$ reflects an increase in the irregularity in the acoustic pathway. The Q factor is defined as the ratio between the resonance frequency and the width of the resonance peak measured at 3 dB below the maximum value (Gómez Álvarez-Arenas, 2003*b*).

The ultrasonic mechanical model

For normal incidence of plane waves on a homogeneous plate, the transmission is made up by the transmitted signal plus the contribution of all the reverberations inside the plate that are, eventually, transmitted to the air at the rear face of the plate. When all these reverberations arrive to the rear face of the plate in phase between them and with the through transmitted signal, a constructive interference is established: the transmitted energy is maximal. This is called a thickness resonance (Gómez Álvarez-Arenas, 2003*a*, 2009*a*). When attenuation in the plate can be considered negligible, then the resonance condition is obtained by:

$$f = m(v_z/2l) \quad (3)$$

where f is the resonant frequency, m is the order of the resonance, and v is the velocity of the ultrasonic longitudinal wave in the plate along the direction normal to the plate (z-axis). For non-normal incidence it is necessary to consider the presence of shear stresses and shear waves in the solid plate.

Spectra of the transmission coefficient of ultrasonic pulses through plant leaves revealed the presence of resonances. Gómez Álvarez-Arenas *et al.* (2009*a*) demonstrated that these resonances are thickness resonances and that there is no evidence of the appearance of shear waves in plant leaves, even when working at non normal incidence. Gómez Álvarez-Arenas *et al.* (2009*b*) shows, for the study of these resonances on leaves, a comparison between a one-layered model and a more detailed model based on a four-layered model (upper epidermis, palisade parenchyma, spongy mesophyll, and lower epidermis). The work demonstrates that, apart from the greater ease in obtaining the data in the one-layered model, the deviation of the one-layer model with respect to the four-layered model for the first thickness resonance (m=1) is very small. Therefore, the one-layer model is a reasonable, accurate, and practical model that has been used in this study as in previous works (Sancho-Knapik *et al.*, 2010).

The macroscopic effective elastic constant (c_{33})

The linearized relationship between the stress (σ) and the strain (γ) produced in an object is given in terms of elastic constants (c) (Auld, 1990):

$$\sigma_i = c_{ij}\gamma_j$$

In this way, c_{33} relates the compressional deformation in the 3 direction with the stress applied in the same direction, an ultrasonic beam in this case (Fig. 1B). c_{33}, named as the macroscopic effective elastic constant of the leaf, represents the elasticity of the whole leaf and it is given in MPa. c_{33} was estimated using equations 1 and 2 and the absolute values of leaf frequency, thickness, and leaf density.

Statistical analysis

The relationship between RWC and f/f_o was adjusted to a four parameter logistic curve

$$\left(f = a+(b-a)/\left(1+(RWC/c)^d\right)\right)$$

for each leaf studied. Although the relationship between RWC and f/f_o for *Q. muehlenbergii* leaves could also be adjusted to a cubic function (<B>=0.99, P <0.0001), the use of the sigmoid function was preferred because the inflexion point is directly inferred from the equation. This function was selected because it describes the evolution between two 'equilibrium states', before and after the turgor loss point.

The relationships RWC versus PLT and RWC versus $1/Q$ were adjusted to a linear segmented model (Schabenberger and Pierce, 2002) for each leaf studied. This is a non-linear model that fit a curve compound of two lineal models with slopes different to zero. The point at which the switch between the two functions occurs is generally called a joint-point, which can easily be associated with a change in the trend of the studied variable during the dehydration process. On the other hand, the relationship between RWC and ρ was adjusted to a square function ($f=a+bx+cx^2$) for each leaf studied.

The turgor loss point was calculated as the inflexion point (coefficient c) of the regression equation for the relationship between RWC and f/f_o. On the other hand, the turgor loss point was associated with the joint-point of the relationships RWC versus PLT and RWC versus $1/Q$. Finally, the turgor loss point was also calculated as the maximum value of the square function for the relationship between RWC and ρ. A Student's t test was used to compare the RWC_{TLP} values obtained from P–V analysis and those recorded from ultrasonic measurements and leaf thickness and density. On the other hand, one-way ANOVAs were performed to compare the evolution of the width and length of the palisade and spongy parenchyma cells as RWC decreased. Multiple comparisons were carried out among the exposition times for the physiological variables using the *post-hoc* Tukey's Honestly Significant Difference test. All statistical analyses were performed with the program SAS version 8.0 (SAS, Cary, NC, USA).

Results

The parameters derived from the pressure–volume curves for *Q. muehlenbergii* are shown in Table 1 and Figs 2 and 3. According to the Höfler diagram (Fig. 2), the symplastic water loss (RWL, %) at the turgor loss point corresponded to 26.6%. Figure 3 shows the strong decrease in the bulk modulus of elasticity (ε, MPa), when turgor pressure (MPa) decreases due to leaf dehydration.

The relationship between the RWC and the percentage of loss of thickness (PLT) was adjusted to a linear segmented model (Fig. 4; <B>=0.93, P <0.0001; all coefficients were statistically significant, P <0.0001). It can be observed that thickness strongly decreases until a certain RWC threshold (0.79±0.03), which is associated with the turgor loss point

Table 1. Parameters derived from the pressure–volume curves for *Quercus muehlenbergii*: water potential at the turgor loss point (Ψ_{TLP}, –MPa), relative water content at the turgor loss point (RWC_{TLP}), maximum bulk modulus of elasticity (ϵ_{max}, –MPa), and maximum turgor (π, –MPa)

Data are mean ±SE.

Quercus muehlenbergii	
Ψ_{TLP} (–MPa)	2.80±0.05
RWC_{TLP}	0.83±0.01
ε_{max} (–MPa)	17.09±0.58
π_0 (–MPa)	2.15±0.07

and close to that derived from P–V curves (Table 1). Once this RWC point is reached, the loss of thickness remains fairly constant. However, leaf density, which was adjusted to a square function (Fig. 5; R^2_{adj}=0.88, P=0.002), shows a slight increase (*c*. 9%) until RWC=0.82±0.01, followed by a slight decrease once this point is exceeded. The loss of leaf thickness is caused by the sharp reduction in the width and length of both spongy and palisade meshophyll cells (Table 2). This process can be observed in the Cryo-SEM micrographs of leaf tissue at full turgor (Fig. 6A, C) and at RWC=0.72 (Fig. 6B, D). Moreover, Fig. 6D shows the buckling experienced by the mesophyll cells when the turgor loss point is exceeded (Fig. 6D).

In Fig. 7 the mean values of f/f_o obtained from ultrasonic measurements are represented against different levels of RWC. The relationship between RWC and f/f_o was adjusted to a four parameter logistic curve (R^2_{adj}=0.99, P <0.0001; all coefficients were statistically significant, P <0.0001), which is characterized by the existence of an inflexion point, corresponding to the turgor loss point (Sancho-Knapik *et al.*, 2010). The turgor loss point for *Q. muehlenbergii* leaves estimated by the standardized frequency corresponded to a RWC of 0.84±0.01. Figure 8 represents the RWC versus the inverse of the quality factor of the leaf first thickness resonance ($1/Q$), which was adjusted to a linear segmented model (R^2_{adj}=0.97, P <0.0001; all coefficients were statistically significant, P <0.0001). The RWC_{TLP} derived from $1/Q$ values was 0.82±0.01. It can be observed

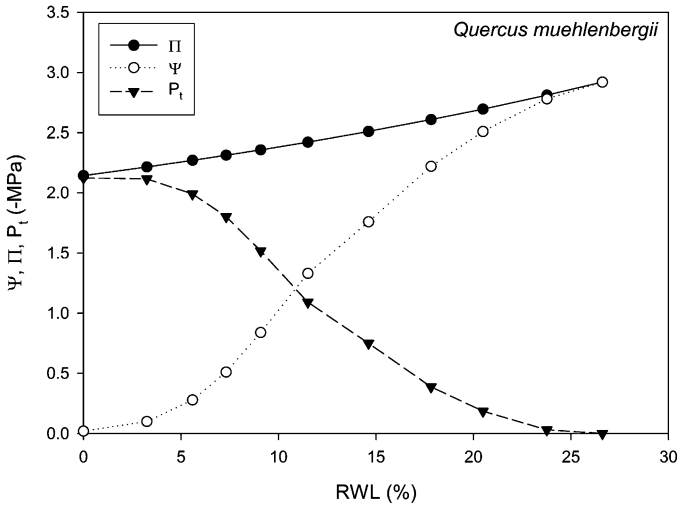

Fig. 2. Höfler diagrams relating symplastic water loss (RWL, %) to turgor pressure (P_t), osmotic potential (π_0), and leaf water potential (Ψ) in *Quercus muehlenbergii*.

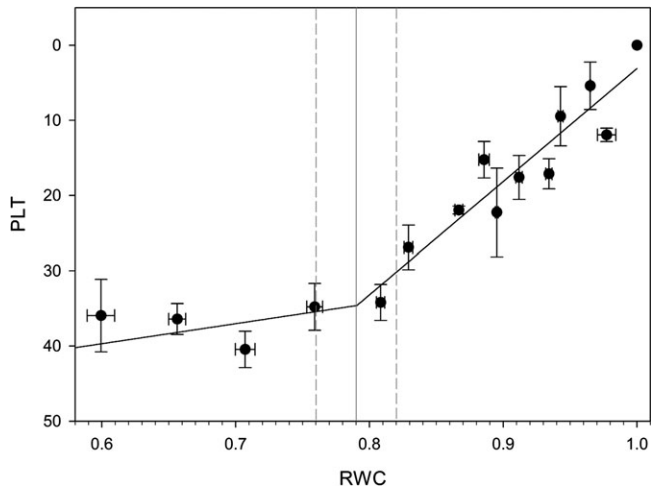

Fig. 3. Relationship between the turgor pressure (MPa) and the bulk modulus of elasticity (ε, MPa) for *Quercus muehlenbergii*. Data are expressed as mean ±SE.

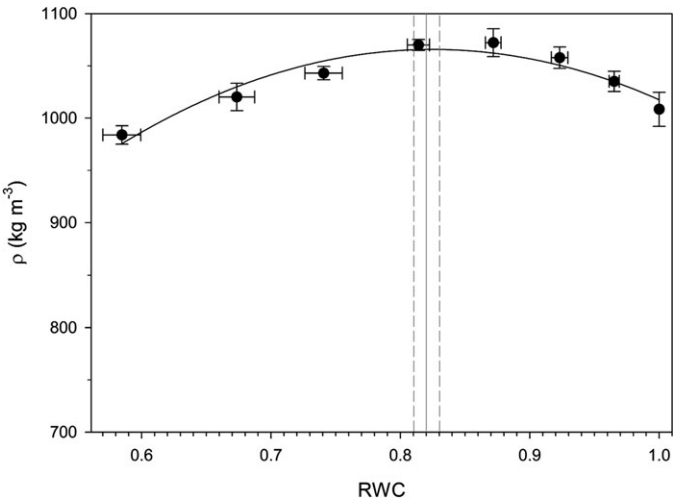

Fig. 4. Relationship between the percentage of loss of thickness (PLT) and the relative water content (RWC) for *Quercus muehlenbergii*. Data are expressed as mean ±SE of ten leaves. Solid line and dashed lines indicates, respectively, the estimated relative water content at the turgor loss point (RWC_{TLP}) and the standard error of this estimation.

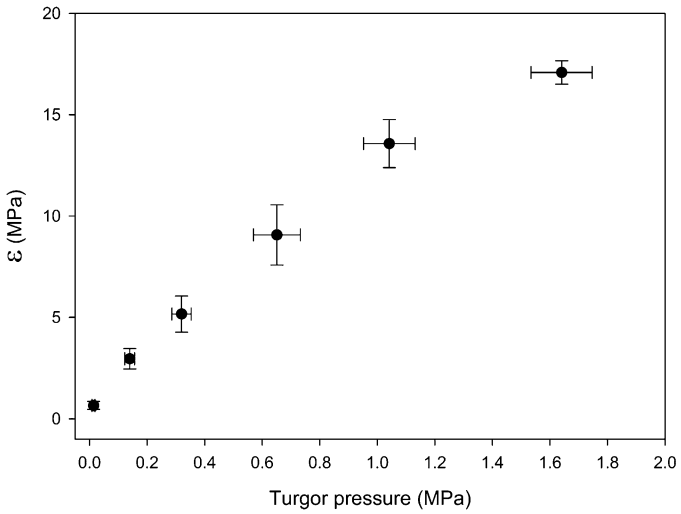

Fig. 5. Relationship between the leaf density (ρ, kg m^{-3}) and the relative water content (RWC) for *Quercus muehlenbergii*. Data are expressed as mean ±SE of ten leaves. Solid line and dashed lines indicates, respectively, the estimated relative water content at the turgor loss point (RWC_{TLP}) and the standard error of this estimation.

that at high RWC values, up to the turgor loss point, $1/Q$ remains nearly constant (*c.* 0.3), while it dramatically increases once this point is exceeded. The results indicate that there is an increase of the attenuation coefficient of ultrasounds, once the leaf is below the RWC threshold determined by the turgor loss point.

The RWC_{TLP} values derived from P–V curves and those estimated from PLT, ρ, and ultrasonic measurements (f/f_o and $1/Q$) were not statistically different at all levels of significance of $P < 0.05$ (Table 3). It should be noted that ultrasonic measurements showed correlation coefficients higher than leaf thickness and density (Table 3).

Figure 9 compares the changes in the bulk modulus of elasticity (ε, MPa) and the estimated macroscopic effective elastic constant (c_{33}) associated with changes in turgor pressure (MPa). Both parameters decreased in a similar way, from full turgor to turgor loss point. However, when turgor is lost, ε was *c.* 0 MPa whereas c_{33} did not reach this value.

Figure 10 shows the influence of the macroscopic effective elastic constant (c_{33}), leaf thickness, and leaf density on the standardized frequency (f/f_o) for *Quercus muehlenbergii* leaves. It can be observed that c_{33} is the main factor affecting the changes in f/f_o. On the other hand, f/f_o was slightly affected by changes in leaf thickness at high f/f_o values (i.e. at high RWC values, before the turgor loss point), whereas leaf density always had a negligible influence on f/f_o values.

Table 2. Width (*x*, μm) and length (*y*, μm) of the palisade and spongy parenchyma cells of *Quercus muehlenbergii* leaves at three different RWC levels

Data are mean ±SE. Different letters within columns indicate significant differences at $P < 0.05$ among the three RWC levels.

RWC	Palisade parenchyma cells		Spongy parenchyma cells	
	x (μm)	*y* (μm)	*x* (μm)	*y* (μm)
1.00	17±1 a	142±1 a	20±1 a	51±3 a
0.83	7±0 b	63±1 b	8±0 b	24±2 b
0.72	6±0 b	53±1 c	8±0 b	16±1 c

Discussion

In this investigation, the changes occurring during different dehydration steps were assessed in terms of ultrasounds measurements, P–V analysis, leaf thickness, leaf density,

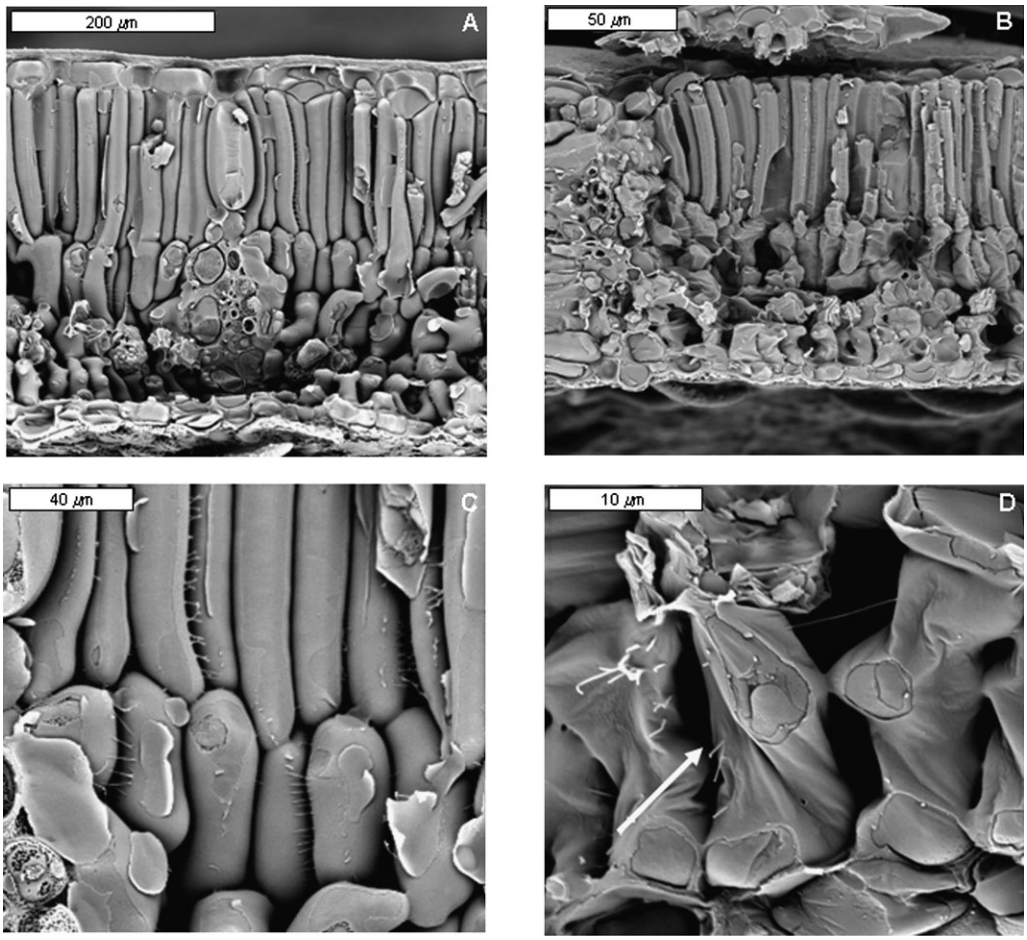

Fig. 6. Cryo-SEM micrographs of leaves of *Quercus muehlenbergii* at full turgor (A, C) and at RWC=0.72 (B, D). White arrow indicates the cell buckling phenomenon.

and leaf structure. Although all the studied parameters were sensitive to changes in plant water status and allowed the estimation of the turgor loss point for *Q. muehlenbergii* leaves (Table 3), most of them showed some drawbacks. Leaf thickness requires contact with the leaf so it is more invasive than the broad-band ultrasonic spectroscopy. Moreover, the absence of changes in leaf thickness after the turgor loss point prevents its use for the estimation of leaf water status beyond this point (Fig. 4). In this way, the variation of leaf density was almost negligible during the

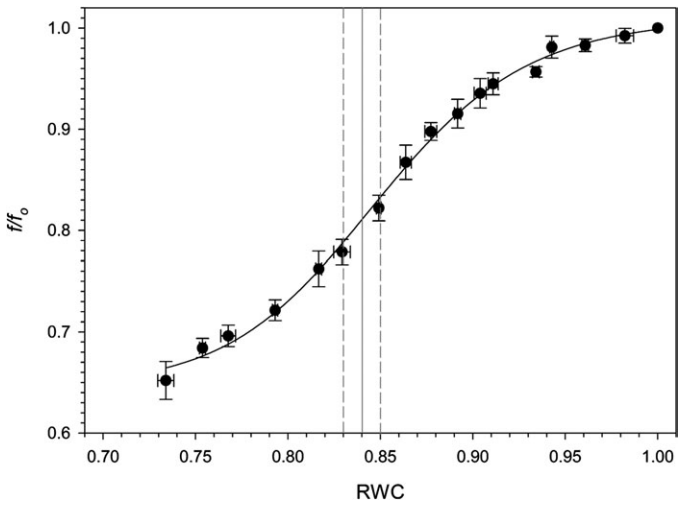

Fig. 7. Relationship between the relative water content (RWC) and the standardized frequency (f/f_o) for *Quercus muehlenbergii*. Data are expressed as mean ±SE of ten leaves. Solid line and dashed lines indicates, respectively, the estimated relative water content at the turgor loss point (RWC_{TLP}) and the standard error of this estimation.

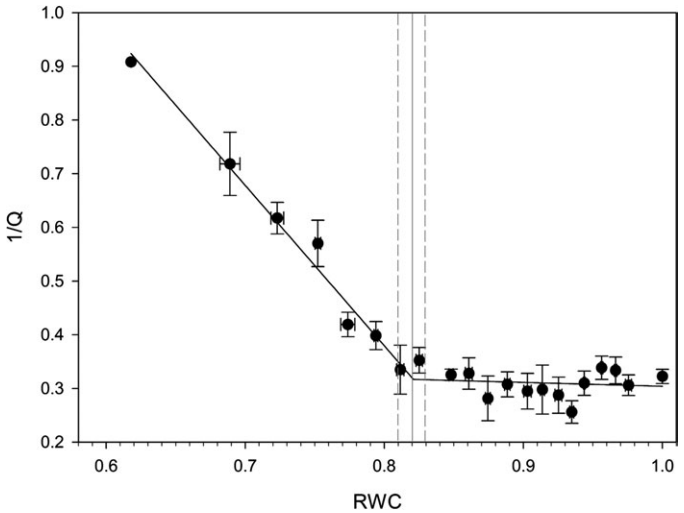

Fig. 8. Relationship between the relative water content (RWC) and the inverse of *Q*-factor (1/*Q*) for *Quercus muehlenbergii*. Data are expressed as mean ±SE of ten leaves. Solid line and dashed lines indicates, respectively, the estimated relative water content at the turgor loss point (RWC_{TLP}) and the standard error of this estimation.

Table 3. Relative water content at the turgor loss point (RWC_{TLP}) estimated from the relationships between RWC and (i) percentage of loss of thickness (PLT), (ii) density (ρ), (iii) standardized frequency (f/f_o), and (iv) the inverse of *Q*-factor (1/*Q*) for *Quercus muehlenbergii* leaves

The adjusted correlation coefficient (R^2_{adj}) and the *P*-value are shown for each studied relationship. All estimated RWC_{TLP} values were not statistically different from RWC_{TLP} derived from P–V curves.

	RWC_{TLP}	R^2_{adj}	*P*
RWC versus PLT	0.79±0.03	0.93	<0.0001
RWC versus. ρ	0.82±0.01	0.88	0.002
RWC versus f/f_o	0.84±0.01	0.99	<0.0001
RWC versus 1/*Q*	0.82±0.01	0.97	<0.0001

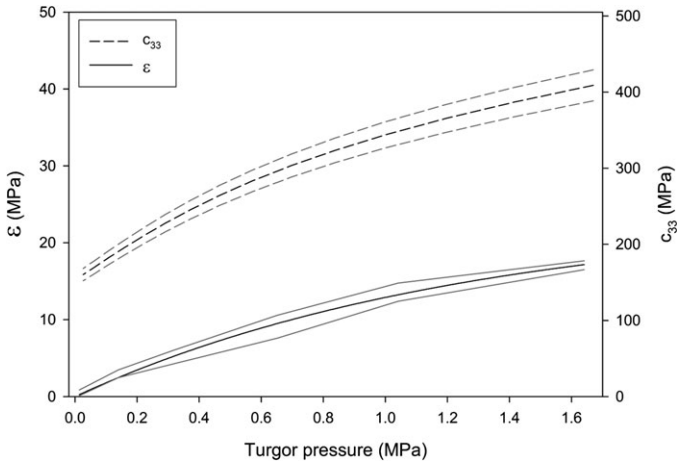

Fig. 9. Relationships turgor pressure (MPa) versus the bulk modulus of elasticity (ϵ, MPa) (solid line) and turgor pressure (MPa) versus the estimated macroscopic effective elastic constant (c_{33}) (dashed line) for *Quercus muehlenbergii*. Grey solid lines and grey dashed lines represent, respectively, the standard errors of ϵ and c_{33}.

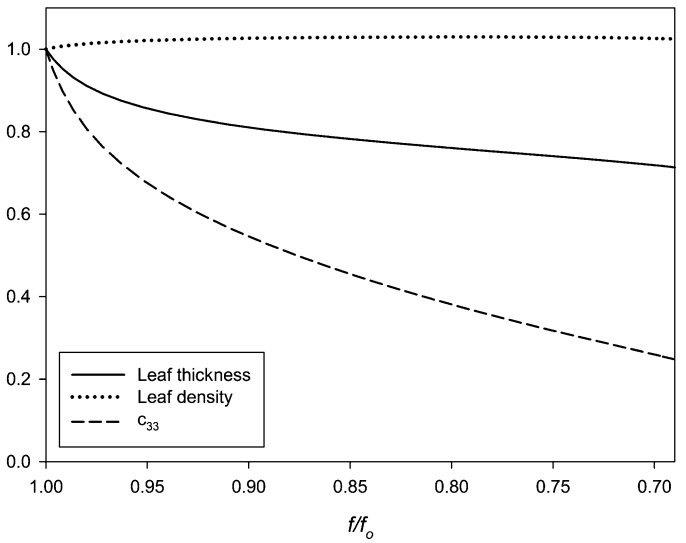

Fig. 10. Variation of the macroscopic effective elastic constant (c_{33}), leaf thickness and leaf density on the standardized frequency (f/f_o) for *Quercus muehlenbergii*. All the variables have been standardized by dividing each value by its value at RWC=1.00.

dehydration process (Fig. 5) due to the existence of compensation between the loss of weight induced by water loss and the reduction in leaf thickness. On the other hand, regarding ultrasonic parameters, the use of the frequency is more suitable than $1/Q$ to estimate plant water status because (i) the frequency is a parameter directly measured while $1/Q$ is a calculated parameter over a certain frequency range, which can be affected by any distortion of the leaf resonance present in the measurement, and (ii) the turgor loss point calculated from frequency data is the inflexion point of a full process of changes (Fig. 7), which is more accurate than the estimation of a point at the beginning of a change process (Fig. 8). For these reasons, it is considered that the frequency is an optimum parameter for the estimation of plant water status. Sancho-Knapik *et al.* (2010) showed that the turgor loss point can be accurately determined by the measurement of the frequency associated with the maximum transmittance. It should be noted that the turgor loss point has been considered a threshold for many physiological processes (Brodribb and Holbrook, 2003; Thomas *et al.*, 2006; Mitchell *et al.*, 2008). Again, no significant differences were found between the RWC_{TLP} derived from analysis of P–V isotherms and those obtained by ultrasounds. The turgor loss point established the separation in two differential phases of the performance of f/f_o as a function of RWC variations.

The first phase, corresponding to high RWC, is characterized by a progressive loss of turgor pressure (Fig. 2), a reduction in the bulk modulus of elasticity of the leaf (ε) (Fig. 3) and a loss of thickness (Fig. 4). The decrease found in ε showed a similar trend to that found for the macroscopic effective elastic constant (c_{33}) of the leaf (Fig. 9). This fact indicates that changes in ε could be associated with changes in c_{33}. It should be noted that ε has been mainly recognized as an indicator of the elastic properties of the cell walls (Tyree and Jarvis, 1982; Saito *et al.*, 2006), whereas c_{33} can be associated with the elasticity of the whole leaf. Thus, there are other factors that could contribute to c_{33}, which may explain the differences found between the values of ε and c_{33} (Fig. 9). This is a matter that deserves further investigations. The decrease in c_{33} (Fig. 9) and the slight increase in ρ (Fig. 5) during the first phase are directly traduced in a reduction of the ultrasound velocity (equation 2) and hence a displacement of the resonance of the leaf towards lower frequencies (equation. 1). This fact could explain the sharp decline found in f/f_o during this first phase (Fig. 7). On the other hand, it can be argued that the f/f_o variations determined could be associated with leaf thickness reductions during leaf dehydration (Fig. 4). However, due to the inverse relationship between thickness and frequencies, higher f/f_o values could theoretically be expected during dehydration (equation 1), while, by contrast, lower f/f_o values were recorded. Therefore, it can be concluded that the changes in c_{33} (that can be attributed to changes in ε) are the main causal factor for the changes found in f/f_o during this first phase, exceeding the effect caused by the loss of thickness during leaf dehydration or density variations (Fig. 10).

The second phase, once the turgor loss point is exceeded, is characterized by the existence of an additional decrease in f/f_o as the leaf dehydration process goes on (Fig. 7), which cannot be caused by changes in the turgor pressure as assumed so far. The further observed reduction of f/f_o beyond the turgor loss point must be justified in terms of a reduction in c_{33}, but now, this c_{33} reduction cannot be produced by the loss of turgor. At the early stages of this procedure, the most likely mechanism is the occurrence of partial elastic buckling of the solid structure (Gibson and Ashby, 1997). This leads to a reduction of c_{33} and hence a reduction of the velocity and a shift of the resonant frequency towards lower frequencies. Therefore, this could explain the further decrease found in the resonant frequency beyond the turgor loss point (Fig. 7). As a first approach to verify this hypothesis, Cryo-SEM micrographs of tissue subjected to differential dehydration stages were obtained and it was indeed observed that water loss induced the occurrence of a high degree of cell shrinkage and stretching (Fig. 6). Around the turgor loss point, both spongy and palisade mesophyll cells experienced a reduction in length and width of *c.* 54% and 59%, respectively. This reduction was more dramatic at 0.72 RWC, where maximum reductions were observed regarding cell length (from 62% to 68%) in contrast to cell width (*c.* 63%). Therefore, it can be concluded that the changes found in f/f_o during this second phase (Fig. 7) are mainly due to the conformational changes of mesophyll cells. Furthermore, these changes caused the formation of large intercellular spaces, which increased the irregularity in the acoustic pathway. This fact may explain the increase of the attenuation coefficient of ultrasounds due to the ultrasound scattering produced by these irregularities and hence the increase of the damping of the leaf thickness (Fig. 8), once the turgor loss point threshold is passed.

Conclusions

In this work c_{33} has been estimated through independent measurements of frequency, thickness, and density. The decrease in c_{33} is the main factor explaining the decrease found in f/f_o before the turgor loss point. The physical changes found in the mesophyll may explain the variations in the ultrasonic properties of the leaf during the second phase. Finally, the knowledge derived from this study can serve for the development of tools for the continuous monitoring of plant water status, in order to maximize water use efficiency in crop plants.

Acknowledgements

This study was partially supported by INIA project SUM2008-00004-C03-03 (Ministerio de Ciencia e Innovación). Financial support from Gobierno de Aragón (A54 research group) is also acknowledged. Work of José Javier Peguero-Pina is supported by a 'Juan de la Cierva'-MICIIN post-doctoral contract.

References

Auld BA. 1990. *Acoustic fields and waves in solids*, 2nd edn. Malabar, FL: Krieger Publishing Company.

Brodribb TJ, Holbrook NM. 2003. Stomatal closure during leaf dehydration, correlation with other leaf physiological traits. *Plant Physiology* **132,** 2166–2173.

Burghardt M, Riederer M. 2003. Ecophysiological relevance of cuticular transpiration of deciduous and evergreen plants in relation to stomatal closure and leaf water potential. *Journal of Experimental Botany* **54,** 1941–1949.

Búrquez A. 1987. Leaf thickness and water deficit in plants: a tool for field studies. *Journal of Experimental Botany* **38,** 109–114.

Christensen RM. 2005. *Mechanics of composite materials*. Dover Publications.

Clifford SC, Arndt SK, Corlett JE, Joshi S, Sankhla N, Popp M, Jones HG. 1998. The role of solute accumulation, osmotic adjustment and changes in cell wall elasticity in drought tolerance in *Ziziphus mauritiana (Lamk)*. *Journal of Experimental Botany* **49,** 967–977.

Corcuera L, Camarero JJ, Gil-Pelegrín E. 2002. Functional groups in *Quercus* species derived from the analysis of pressure–volume curves. *Trees, Structure and Function* **16,** 465–472.

Gibson LJ, Ashby MF. 1997. *Cellular solids*. Cambridge University Press.

Gómez Álvarez-Arenas TE. 2003*a*. Air-coupled ultrasonic spectroscopy for the study of membrane filters. *Journal of Membrane Science* **213,** 195–207.

Gómez Álvarez-Arenas TE. 2003*b*. A nondestructive integrity test for membrane filters based on air-coupled ultrasonic spectroscopy. *IEEE Transactions on Ultrasonics, Ferroelectrics and Frequency Control* **50,** 676–685.

Gómez Álvarez-Arenas TE. 2004. Acoustic impedance matching of piezoelectric transducers to the air. *IEEE Transactions on Ultrasonics, Ferroelectrics and Frequency Control* **51,** 624–633.

Gómez Álvarez-Arenas TE, Sancho-Knapik D, Peguero-Pina JJ, Gil-Pelegrín E. 2009*a*. Noncontact and noninvasive study of plant leaves using air-coupled ultrasounds. *Applied Physic Letters* **95,** 193702.

Gómez Álvarez-Arenas TE, Sancho-Knapik D, Peguero-Pina JJ, Gil-Pelegrín E. 2009*b*. Determination of plant leaves water status using air-coupled ultrasounds. *IEEE International Ultrasonics Symposium Proceedings* 771–774.

Larcher W. 2003. *Physiological plant ecology. Ecophysiology and stress physiology of functional groups*. Berlin, Heidelberg, New York: Springer-Verlag.

McBurney T. 1992. The relationship between leaf thickness and plant water potential. *Journal of Experimental Botany* **43,** 327–335.

Mitchell PJ, Veneklass EJ, Lambers H, Burgess SSO. 2008. Leaf water relations during summer water deficit: differential responses in turgor maintenance and variation in leaf structure among different plant communities in south-western Australia. *Plant, Cell and Environment* **31,** 1791–1802.

Ogaya R, Peñuelas J. 2006. Contrasting foliar responses to drought in *Quercus ilex* and. *Phillyrea latifolia. Biologia Plantarum* **50,** 373–382.

Pritchard J. 2007. Plant tissues and cells: turgor pressure. In: Roberts K, ed. *Handbook of plant science*, Vol. I. Chichester, England: Wiley, 148–151.

Saito T, Soga K, Hoson T, Terashima I. 2006. The bulk elastic modulus and the reversible properties of cell walls in developing *Quercus* leaves. *Plant and Cell Physiology* **47,** 715–725.

Sancho-Knapik D, Gómez Álvarez-Arenas T, Peguero-Pina JJ, Gil-Pelegrín E. 2010. Air-coupled broadband ultrasonic spectroscopy as a new non-invasive and non-contact method for the determination of leaf water status. *Journal of Experimental Botany* **61,** 1385–1391.

Schabenberger O, Pierce FJ. 2002. *Contemporary statistical models for the plant and soil sciences*. Boca Raton, FL: CRC Press, 252–259.

Temkin S. 1981. Elements of acoustics. New York: John Wiley & Sons.

Thomas TR, Matthews MA, Shackel KA. 2006. Direct *in situ* measurement of cell turgor in grape (*Vitis vinifera* L.) berries during development and in response to plant water deficits. *Plant, Cell and Environment* **29,** 993–1001.

Tyree MT. 1976. Negative turgor pressure in plant cells: fact or fallacy? *Canadian Journal of Botany* **54,** 2738–2746.

Tyree MT, Hammel HT. 1972. The measurement of the turgor pressure and the water relations of plants by the pressure-bomb technique. *Journal of Experimental Botany* **23,** 267–282.

Tyree MT, Jarvis PG. 1982. Water in tissues and cells. In: Lange OL, Nobel PS, Osmond CB, Ziegler H, eds. *Encyclopedia of plant physiology, New series*, Vol. 12b. Berlin: Springer-Verlag, 35–77.

Vilagrosa A, Bellot J, Vallejo VR, Gil-Pelegrín E. 2003. Cavitation, stomatal conductance, and leaf dieback in seedlings of two co-occurring Mediterranean shrubs during an intense drought. *Journal of Experimental Botany* **54,** 2015–2024.

Zimmermann D, Reuss R, Westhoff Gebner P, Bauer W, Bamberg Bentrup FW, Zimmermann U. 2008. A novel, non-invasive, online-monitoring, versatile and easy plant-based probe for measuring leaf water status. *Journal of Experimental Botany* **59,** 3157–3167.